Journal of Sciences, Islamic Republic of Iran 18(3): 239-251 (2007) http://jsciences.ut.ac.ir
University of Tehran, ISSN 1016-1104

The Analysis of Paragenesis of Mn-Silicate Bearing Quartzites and Schists in Highly Oxidized Blueschist Facies by Korzhinsky and Schrienemakers' Methods

J. Izadyar*

Department of Geology, Faculty of Sciences, Zanjan University, Zanjan, Islamic Republic of Iran

Abstract

By Korzhinsky and Schrienemakers' methods, phase relations of Mn-Al-Ca-silicates and other minerals in highly oxidized quartzites and schists of blueschist type metamorphism have been discussed. Because, such rocks were extensively studied in central Shikoku of Japan and in Andros and Evvia islands of Greece, they have been considered as thermodynamic system for discussion. The system contains piemontite, braunite, surssasite, spessartine, pumpellyite, phlogopite, clinochlore, talc and kyanite with excess muscovite, quartz and water. System components include Al_2O_3, Mn_2O_3, MnO, CaO, MgO and K_2O with excess SiO_2 and H_2O. Application of Korzhinsky and Schrienemakers' methods into the system gives three independent petrogenetic girds. Considering the chemographic relationships in the petrogenetic gird of [Su]-[Tlc]-[Pi], it can vividly be concluded that highly oxidized Mn-bearing quartzites or schists in blueschist facies divided to low temperature assemblage (Su + Pmp + Clin + Pi), medium temperature assemblage (Clin + Sps + Bru + Pi) and high temperature assemblage (Tlc + Sps + Br + Pi). Application to natural assemblages, show correspondence between different natural assemblages in response to variable physical conditions and their relative stability predicted from Korzhinsky and Schrienemakers' methods.

Keywords: Andros and Evvia islands of Greece; Central Shikoku of Japan; Blueschist facies; Mn-bearing silicates; Highly oxidized quartzites and schists

1. Introduction

Highly oxidized, aluminous manganese-rich schists and quartzites have been frequently reported in high-pressure metamorphic belts, for example in Europe [24,33], New Zealand [19] and Japan [18]. According to Chopin's definition [30] in oxidized assemblage, Mn is dominantly trivalent in the minerals such as braunite, piemontite, ardenite and phengite and also spessartine incorporates all available Mn^{2+} and hematite is the characteristic iron-bearing phase. Most petrological studies on natural assemblages of Mn-Al-Ca-silicates focused on their unusual mineral composition and on cation partitioning between their minerals [9,18-20,33].

*E-mail: izadyar@znu.ac.ir

Experimental investigations petinent to Mn-Al-Ca-silicates in piemontite schists and related rocks have been performed with respect to the P-T-X-fo_2-stabilities of piemontite [3,4,21,22], spessartine [15,29] and braunite [2]. Reinecke [32] by studying on highly oxidized, low-grade quartzites from Andros and Evvia islands, Greece, discussed the phase relations among piemontite, sursassite, braunite, spessartine, chlorite, quartz, phengite, phlogopite and hematite. Izadyar *et al.* [16,17] discussed the phase relations of piemontite-quartz schists from the intermediate and high-grade part of the Sanbagawa metamorphic belt. Detailed field study, petrographic and microprobe data on Mn-bearing schists and quartzites from Sanbagawa metamorphic belt, Japan [16-18] and Andros and Evvia islands, Greece [32,33] provide the best opportunity to widen over knowledge of such rocks as indicators of equilibration within the high-pressure facies sequence. To understand the stability of Mn-Al-Ca-silicates in response to changes in temperature and pressure, an attempt is made to generalize the low to high-grade paragenetic evolution of Mn-Al-Ca-silicate assemblages and related minerals by producing a petrogenetic gird by Korzhinsky and Schrinemakers' methods and to apply it to similar assemblages reported from other occurrences of the world.

2. Geological Setting

The Sanbagawa metamorphic belt is an area in Southwest Japan that was subjected to a Cretaceous regional metamorphism of intermediate high pressure (Fig. 1a). The belt is bounded to the north by the Ryoke belt, a Cretaceous low pressure regional metamorphic belt. The two metamorphic belts are separated by a major fault, the Median Tectonic Line (MTL) [5,34]. A large proportion of the Sanbagawa belt consists of metapelites interbeded with varying amounts of oceanic crustal material and is accompanied by ultramafic and mafic tectonic blocks in the highest grade part of central Shikoku [34]. Quartz schists, *e.g.* manganiferous and ferruginous metacherts, are common in the schists [5]. In central Shikoku, the Sanbagawa metamorphic belt is widest and can be divided into four mineral zones; chlorite, garnet, albite-biotite and oligoclase-biotite zones, based on the appearance of index minerals in pelitic schists [12,10,5]. Metamorphic conditions in this area were estimated at 250-300°C and 5-6 kbar for the lower chlorite zone, and 610°C and 10-12 kbar for the oligoclase-biotite zone [5]. Thus, the overall slope of the P-T trajectory from chlorite zone to the albite-biotite zone is positive (prograde path of metamorphism), but chemical zonation of some minerals such as amphibole and garnet suggest also a retrograde path [5]. In central Shikoku, the highest-grade metamorphic zone occurs in the middle of the structural sequence, the metamorphic grade decreasing both upward and downward [5]. Banno and Sakai [5] interpreted this structure as a large-scale post-metamorphic recumbent fold. Piemontite-quartz schists form centimeter to meter thick layers, and are commonly in direct contact with pelitic and basic schists. Some of them are interbeded with the quartz-rich layers without piemontite, forming well-defined banding which corresponds to the original sedimentary bedding [16]. For further details on the petrology of the Sanbagawa piemontite-quartz schists, the reader is referred to Izadyar [16-18].

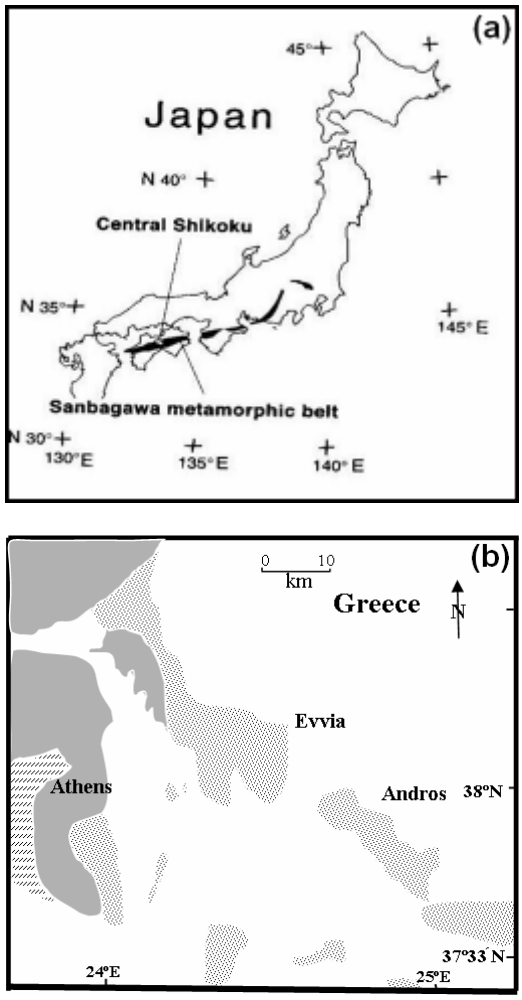

Figure 1. a) Regional distribution of the low-temperature, high-pressure Sanbagawa metamorphic belt, Japan (after Izadyar [17]); b) Regional occurrences of blueschist type metamorphic rocks (stippled) in Evvia and Andros, Greece. Horizontal ruling = predominantly carbonatic rocks (after Reinecke [32]).

Table 1. Mineral names, abbrivations, volumes and entropies of the system phases. Thermodynamic data were adapted from Holland and Powell [14] and Reinecke [32]. Most of the abbreviations are following Kretz [23]

Sanbagawa (Japan)	Andros (Greece)	Evvia (Greece)
quartz+piemontite+braunite+talc+ spessartine+phlogopite+hematite+ chlorite+phenigite+albite	quartz+piemontite+braunite+ spessartine+hematite+chlorite+ phenigite	quartz+piemontite+sursassite+ braunite+hematite+chlorite
quartz+piemontite+braunite+ talc+spessartine+albite+ hematite+chlorite+phenigite	quartz+piemontite+spessartine+ braunite+hematite+phlogopite+ ardenite	quartz+piemontite+sursassite+ hematite+chlorite+phengite
quartz+piemontite+braunite+ spessartine+albite+hematite+ chlorite+phenigite	quartz+piemontite+spessartine+ braunite+chlorite+phlogopite+ ardenite+phengite	quartz+piemontite+braunite+ chlorite

Metamorphic rocks on Andros and Southern Evvia form part of the Eocene blueschist belt of the Attic-Cycladic crystalline complex (Fig. 1b). They consist of Paleozoic to presumed Mesozoic metapelitic, calcareous, or quartzose schists, metabasic schists, various types of marbles and minor intercalations of meta-acidic tuffs as well as Mn- and or Fe-rich quartzites [31,32]. In Southern Evvia, Mn-rich quartzitic rocks are intercalated into a sequence of marbles, calcareous metapelitic schists and schistose quartzites [32]. The Mn-rich rocks are a few meters up to tens of meters thick and typically consist of platy piemontite quartzites, braunite quartzites and micaschists rich in piemontite. They are associated with hematite-rich quartzites and massive brown and red metaradiolarites [32]. On Andros, the Mn-rich quartzites are texturally and chemically similar to those of Southern Evvia, but of higher metamorphic grade. Piemontite and spessartine bearing quartzites form centimeter to meter thick beds within a sequence of isoclinally folded phengite-chlorite quartzites, subordinate greenschists and impure marbles. On Evvia, the common occurrence of lawsonite(±albite), pumpellyite, and aegirine-jadeite + quartz indicate that the physical conditions of high-pressure, low-temperature metamorphism have been lower than T = 400°C at minimum pressures of about 8-9 kbars. High-pressure assemblages were overprinted at reduced pressures within the stability field of pumpellyite (T < 390°C at 8 kbar and < 370°C at 5 kbar leading to assemblages with albite, epidote, chlorite, pumpellyite, quartz, calcite, titanite and rare biotite and stilpnomelan [32,33]. On central Andros, the presence of omphacite / aegirine-jadeite + quartz, deerite + magnetite + quartz, and phengite with Si-values near 3.42 (per 12 O + OH) in quartzites indicates pressures in excess of 10 kbar at maximum temperature of 450 to 500°C for the high-pressure metamorphism [32,33,26]. Pumpellyite and lawsonite have not been found in a wide range of bulk rock compositions. Thus, the metamorphic temperature may have been higher by ≈ 50 to 100°C on Andros than on Evvia. Later overprinting on Andros occurred at greenschist facies conditions (T ≈ 400-500°C) [32,33]. For further details on the geology and petrology of the areas, the reader is referred to Reinecke [31-33].

3. Petrography and Mineral Chemistry

Piemontite-quartz schists from central Shikoku commonly show compositional banding with alternating piemontite-rich and quartz-rich bands. The width of the piemontite-rich bands ranges from 0.5 to 1.5 mm. They are mainly composed of piemontite, garnet, talc and hematite with subordinate amounts of quartz, phengite, albite and braunite. The quartz-rich bands (1-2 mm thick) mostly contain quartz, phengite, albite, talc and chlorite with minor amounts of piemontite, garnet, hematite and braunite. The mineral parageneses of Sanbagawa piemontite-quartz schists are listed in Table 1.

Piemontite quartzites on Evvia and Andros typically show a millimeter- to centimeter-scale compositional banding resulting from variable proportions of quartz to fine-grained surssasite, piemontite, braunite, ardennite, phengite, garnet and hematite [32]. The characteristic low-variance assemblage of piemontite quartzites on Evvia is: quartz, piemontite, surssasite, braunite,

hematite and chlorite. More frequently, sub-assemblages with combinations of 1 to 3 phases in addition to quartz and chlorite occur (Table 1). Accessory crosstie, phengite, ardennite, rutile, titanite, albite, apatite, Na-pyroxene and tourmaline are present in a few samples. Piemontite-spessartine and braunite quartzites on Andors are characterized by the assemblage: quartz, piemontite, spessartine, braunite, hematite, chlorite, rutile and phengite (Table 1). Accessory minerals are crosstie, ardenite, albite, tourmaline, apatite and rare titanite [31,32].

On Andros and Evvia, piemontite froms euhedral to subhedral prismatic grins and it contains 14-26% piemontite and 12-20% pistacite endmembers. In the Sanbagawa, piemontites are present in the matrix as well as enclosed by garnet and albite in piemontite-rich and quartz-rich bands. In piemontites, two zones can be distinguished. Core often forms large crystals and outer zone is narrow rim surrounding the core. The chemical analyses of piemontites from mentioned area are tabulated in Tables 2 and 3 [17,32,33].

Table 2. Representative analyses of piemontite (Pi), garnet (Grt), chlorite (Chl), talc (Tlc), phlogopite (Phl) and phengite (Phn) from Sanbagawa piemontite-quartz schists (After Izadyar [17])

Sample No.	**1510-0**	**1510-0**	**1510-0**	**1510-0**	**1510-0**	**1510-0**
Mineral Name	**Pi**	**Grt**	**Chl**	**Tlc**	**Phl**	**Phn**
Point No.	**5112**	**27**	**113**	**156**	**1415**	**38**
SiO_2	37.74	37.39	30.05	63.15	44.61	48.72
TiO_2	0.11	0.23	0.09	-	-	0.52
Al_2O_3	20.55	19.58	20.43	-	11.15	26.43
Fe_2O_3	2.9	1.74	0.67	0.07	0.81	4.17
Mn_2O_3	14.58	-	0.08	-	-	0.39
MnO	-	36.92	-	0.33	1.12	-
MgO	-	0.71	32.65	30.96	24.8	3.13
CaO	22.19	4.08	0.07	-	-	-
Na_2O	-	-	-	-	-	0.55
K_2O	-	-	-	-	10.12	9.7
Total	98.78	100.63	84.04	94.51	92.61	93.61
	12.5	12	28	22	22	22
Si	3	3	5.77	8	6.36	6.64
Ti	-	-	0.01	-	-	0.05
Al^{IV}	1.94	1.86	2.28	-	1.64	1.36
Al^{VI}	0.01	0.01	0.01	-	0.23	2.88
Fe^{3+}	0.18	0.09	0.09	0.007	0.09	0.43
Mn^{2+}	-	2.55	-	0.03	0.13	-
Mn^{3+}	0.88	-	0.01	-	-	0.04
Mg	-	0.08	9.34	5.87	5.27	0.64
Ca	1.96	0.34	0.01	-	-	-
Na	-	-	-	-	-	0.15
K	-	-	-	-	1.84	1.68
Total	7.89	7.97	19.86	13.9	15.57	13.87

Table 3. Representative analyses of piemontite (Pi), garnet (Grt), surssasite (Su0, braunite (Bru), phengite (Phn) and phlogopite (Phl) from Evvia and Andros (After Reinecke [32,33])

Sample No.	**801179**	**79-255**	**80-29**	**80-16**	**83-44**	**80-84**
Mineral Name	**Pi**	**Su**	**Bru**	**Phn**	**Phl**	**Grt**
SiO_2	37.3	35.2	10.2	49.5	42.8	36.5
TiO_2	-	0.07	0.12	0.1	0.11	0.1
Al_2O_3	22.9	21.9	0.36	26.2	13.9	19.6
Fe_2O_3	11.4	1.8	7.7	3.8	0.7	1.8
Mn_2O_3	1.9	-	81.3	-	-	-
MnO	-	26.8	-	0.16	3.8	35.6
MgO	-	2.8	0.07	3.5	23.6	-
CaO	23.8	3.8	0.4	-	-	6.3
Na_2O	-	-	-	0.48	0.08	-
K_{2O}	-	-	-	10.4	10	-
Total	97.3	92.37	100.1	94.14	95	99.4
	12.5	16	8	22	22	12
Si	2.99	6	1.03	6.71	6.03	2.98
Ti	-	0.01	0.01	0.01	0.01	0.006
Al^{IV}	-	-	-	1.29	1.97	-
Al^{VI}	2.168	4.42	0.04	-	0.34	1.89
Fe^{3+}	0.686	0.23	0.58	0.39	0.07	0.11
Mn^{2+}	-	3.27	-	-	0.45	2.46
Mn^{3+}	0.116	0.62	5.3	-	-	-
Mg	-	0.72	0.01	0.71	4.95	-
Ca	2.04	0.7	0.04	-	-	0.55
Na	-	-	-	0.13	0.02	-
K	-	-	-	1.8	1.8	-
Total	8	13	8	11	15.64	8

Sursassite occurs as prismatic blades and more rarely as fibrous crystals in Evvia and Andros and their representative analyses are shown in Table 3. Sursassite is not present in the Sanbagawa samples [32,33].

In piemontite quartzties on Andros, spessartine forms isometric grains which are in apparent textural equilibrium with piemontite, hematite, braunite, chlorite, phengite, rutile and crosstie but in spessartine quartzites it forms an equigranular texture or occurs as large poikiloblasts which overgrow pre-existing braunite, piemontite, quartz, hematite and rutile. Similar textures have been observed of those samples from Evvia in which spessartine has been formed by decomposition of surssasite. Garnets in the Sanbagawa are euhedral and their size ranges from 1 to 3 mm. Sometimes, they occur as poikiloblasts, containing many inclusions of piemontite, quartz, hematite, braunite, talc and amphibole. Chemically, these garnets are homogenous Ca-Fe-bearing spessartine. Their chemical compositions are shown in Tables 2 and 3 [17,32,33].

In the Evvia and Andros Na-amphibole form prismatic colorless crystals up to 2 mm long or sheaves of prismatic crystals aligned in the foliation. In general, the Na-amphiboles are typically Mg-rich crossite. In the Sanbagawa samples, colorless amphiboles occur only as inclusions in albite and garnet porphyroblasts and their composition corresponds to crossite. In high grade of the Sanbagawa, amphiboles occur as matrix grains with a tabular shape and their composition are magnesian-kathophorite or barroisite [17,32,33].

Phengite from Evvia and Andros show considerable $SiMgAl_{-1}Al_{-1}$ substitution (Table 3). Phengite is present in all examined rocks in the Sanbagawa and is usually a matrix phase in association with the other phases. Representative analyses of phengites are tabulated in Tables 2 and 3 [17,32,33].

In the Evvia and Andros, talc could not be detected but in the piemontite-quartz schists of the Sanbagawa talc occurs as tabular aggregates or as intercalations with phengite or chlorite and its composition is very close to the ideal formula (Table 2) [17].

Phlogopite is exclusively present in braunite-spessartine bearing assemblage on Andros (Tables 2 and 3). Minor phlogopite occurs at the margin of phengite in the Sanbagawa samples but it is not in contact with either chlorite nor talc [17,32,33].

Colorless chlorite is a ubiquitous though subordinate constituents of most assemblage from Evvia and Andros and chemically are aluminous clinochlore. Chlorites in the higher-grade metamoprphic rocks on Andros appear to have higher Al^{IV} and lower Si contents than chlorites from Evvia. Chlorite is the major constituent mineral in the Sanbagwa samples. It is commonly found with parallel growth of talc, phengite and talc with sharp contacts. The average composition of analyzed chlorite is close to ideal clinochlore end-member but some deviation from clinochlore through $MgSiAl_{-1}Al_{-1}$ substitution can be seen (Table 2) [17,32,33].

Plagioclase is present in Evvia, Andros and Sanbagawa samples and chemically is close to pure albite. In the Sanbagawa, albite is porphyroblast phase and contains many inclusion of hematite, talc, phengite, amphibole, piemontite and quartz [17,32,33].

Braunite from Evvia and Andros is concentrated in layers on aggregates of subhedral crystals which are intimately intergrown with quartz, or it is randomly interspersed as microcrystalline particles among coarser crystalline quartz, piemontite and surssasite (Table 3). In the Sanbagawa, braunite usually occurs in quartz-rich and piemontite-rich bands and rarely as inclusions in the albite and garnet [17,32,33].

Hematite occurs in the matrix and as inclusion in albite and garnet and its average chemical composition is $(Fe_{1.9}Mn_{0.8}Ti_{0.01})O_3$ [17,32,33].

4. Phase Relations

In the following, the phase relations among piemontite (Pi), braunite (Bru), sursassite (Su), spessartine (Sps), pumpellyite (Pmp), phlogopite (Phl), clinochlore (Clin), talc (Tlc) and kyanite (Ky) with excess muscovite, quartz and water have been discussed. Chemical representation of these assemblages involves the components Al_2O_3, Mn_2O_3, MnO, CaO, MgO, K_2O ($AMn^{3+}Mn^{2+}CMk$) with excess SiO_2 and H_2O (Tables 2 and 3). Iron presents mostly as Fe^{3+} in hematite and sodium in albite. Graphical presentation of the assemblage is shown by projection from muscovite + quartz + H_2O into the Mn-Ca-Al-Mg-K Space (Fig. 2). In order to represent Mn^{3+} + Mn^{2+} as Mn^{total}, in projection of piemontite, surssasite and braunite, it is assumed that fO_2 in the fluid phase of each assemblage in each diagram is fixed. Mineral names, chemical compositions, abbreviations, volumes and entropies of the relevant minerals are tabulated in Table 4. Based on Gibbs phase rule, an invariant point for a 6-component system in P-T field requires that eight phases be in equilibrium, and a univariant line requires seven phases. For the general case, with 9 phases (spessartine, piemontite, surssasite, pumpellyite, braunite, phlogopite, clinochlore, talc and kyanite) in the AMn^{3+} Mn^{2+} CMK, taken eight at a time, there will be nine invariant points. They are represented by an abbreviation in Table 5. As an invariant point involves eight of the nine phases, the abbreviation of invariant

point is designated by brackets, which contain one abbreviation for phase not involved. For the general case with nine phases taken seven at a time, there will be 36 univariant lines (Table 5). However, this system contains many linear and planar degeneracies, therefore, the univariant lines reduce to 18. The invariant points, 18 univariant reactions and univariant assemblages are tabulated in Table 5. Stoiqiometric univariant reactions are also presented in Table 6. It should be noted that, because of many degeneracies in the system and insufficient thermodynamic data of the phases, it is almost impossible to use of thermodynamic softwares such as THERMOCALC or TWEEQU to find metamorphic reactions in the system.

Therefore, complete set of metamorphic reactions were obtained using following method. For obtaining univariant reactions around an invariant point, at first a compositional determinant has been built in which rows are coefficients of phase compositions involved in the system (spessartine, piemontite, surssasite, pumpellyite, braunite, phlogopite, clinochlore, talc and kyanite) based on the system components (Al_2O_3, Mn_2O_3, MnO, CaO, MgO, K_2O, SiO_2 and H_2O). In the constructed determinant, excess phases (quartz, muscovite and water) and excess system component (SiO_2, H_2O) have not shown.

	Al_2O_3	MgO	CaO	MnO	Mn_2O_3	K_2O
Br	0	0	0	1	3	0
Su	2	1	0	4	0.5	0
Sps	1	0	0	3	0	0
Pmp	1	0.5	4	0.5	1.5	0
Phl	0.5	3	0	0	0	0.5
Clin	1	5	0	0	0	0
Tlc	0	3	0	0	0	0
Ky	1	0	0	0	0	0
Pi	1	0	2	0	0.5	0

In braunite absent invariant point, the compositional determinant is:

Su	2	1	0	4	0.5	0
Sps	1	0	0	3	0	0
Pmp	1	0.5	4	0.5	1.5	0
Phl	0.5	3	0	0	0	0.5
Clin	1	5	0	0	0	0
Tlc	0	3	0	0	0	0
Ky	1	0	0	0	0	0
Pi	1	0	2	0	0.5	0

For finding univariant reactions in the braunite absent determinant, it should be proceed by following way:

[Su] =

Sps	1	0	0	3	0	0
Pmp	1	0.5	4	0.5	1.5	0
Phl	0.5	3	0	0	0	0.5
Clin	1	5	0	0	0	0
Tlc	0	3	0	0	0	0
Ky	1	0	0	0	0	0
Pi	1	0	2	0	0.5	0

Then, the determinant was expanded by considering every phase in determinant:

Sps

1	0.5	4	0.5	1.5	0
0.5	3	0	0	0	0.5
1	5	0	0	0	0
0	3	0	0	0	0
1	0	0	0	0	0
1	0	2	0	0.5	0

− Pmp

1	0	0	3	0	0
0.5	3	0	0	0	0.5
1	5	0	0	0	0
0	3	0	0	0	0
1	0	0	0	0	0
1	0	2	0	0.5	0

+ Phl

1	0	0	3	0	0
1	0.5	4	0.5	1.5	0
1	5	0	0	0	0
0	3	0	0	0	0
1	0	0	0	0	0
1	0	2	0	0.5	0

− Clin

1	0	0	3	0	0
1	0.5	4	0.5	1.5	0
0.5	3	0	0	0	0.5
0	3	0	0	0	0
1	0	0	0	0	0
1	0	2	0	0.5	0

+ Tlc

1	0	0	3	0	0
1	0.5	4	0.5	1.5	0
0.5	3	0	0	0	0.5
1	5	0	0	0	0
1	0	0	0	0	0
1	0	2	0	0.5	0

− Ky

1	0	0	3	0	0
1	0.5	4	0.5	1.5	0
0.5	3	0	0	0	0.5
1	5	0	0	0	0
0	3	0	0	0	0
1	0	2	0	0.5	0

+ Pi

1	0	0	3	0	0
1	0.5	4	0.5	1.5	0
0.5	3	0	0	0	0.5
1	5	0	0	0	0
0	3	0	0	0	0
1	0	0	0	0	0

Calculation on mentioned determinant gives following surssasite absent univariant reaction for the braunite absent invariant point:

7.5 Tlc + 4.5 Ky == 4.5 Clin

This process should be repeated in the same way for spessartine, pumpellyite, phlogopite, clinochlore, talc, kyanite and piemontite to complete univariant reactions around braunite absent invariant point. The same procedure should be applied for other invariant points in the system which are: [Su], [Sps], [Pmp], [Phl], [Clin], [Tlc], [Pi] and [Ky].

Morey-Schreinemakers' rule decides the topology of invariant reaction lines radiating from each invariant point [35]. Zen [35] depicted the correlation between the topology of invariant reaction lines around a univariant point and the chemographic relation of phases composing the invariant assemblage for the three component system. This method provides two possible cases of topology which are related in mirror image. The slope of the univariant reaction lines in the P-T field can be calculated using a series of approximations. These assumptions may harm to discuss the exact stability field of minerals but is still effective to calculate and predict the stability field so far as in the semi-quantitative model, we are mainly interested in the topology of the univariant lines around invariant points of the petrogenetic girds.

This procedure decides a unique topology around an invariant point, and reduces the number of the possible

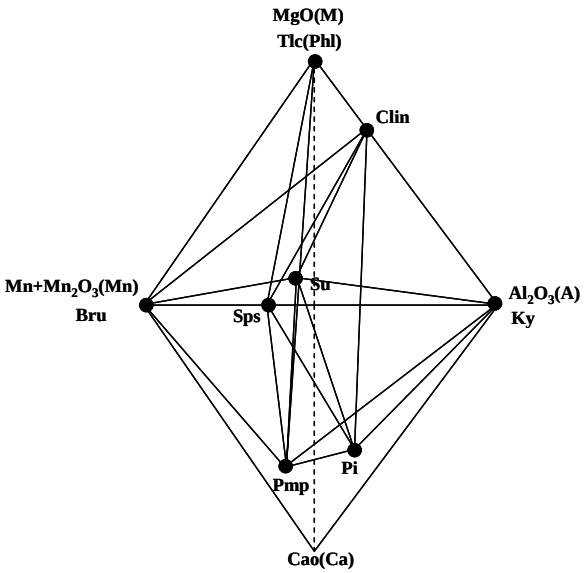

Figure 2. Al_2O_3-Mn_2O_3/MnO-CaO-MgO(ACMMn) tetrahedral diagram showing projection points of minerals in the system with excess quartz, muscovite and H_2O.

petrogenetic grids by half. Considering a typical dehydration reaction:

$$A_s + B_s = C_s + D_s + n\,(H_2O)_f$$

where the subscript "s" indicates a solid phase and the subscript "f" indicates a fluid phase which is assumed herein to be pure H_2O. The slope is given by the equation:

$$\left(dp/dT\right)_{G=0} = \frac{\Delta S}{\Delta V_s + n\left(H_2O\right)\, V_{H_2O}\, \left(dp_{H_2O}/dp_s\right)}$$

where P_s, ΔV_s and ΔS represent the solid pressure, the change in volume of solid phase and the change in entropy respectively, V_{H2O} is the molar volume of water at specified P_{H2O} and T and n(H_2O) is the number of moles of H_2O given by the reaction. Assuming that the change of the molar volume of the solid phases with the change of P-T conditions is negligible small, the molar volumes of the solid phases are referred to those at the standard state (Table 4).

V_{H2O} was taken as 19.8 cc/mole, the value at 350°C and 3.5 kbar [6], because this value roughly represents the median of V_{H2O} under the P-T range considered.

Entropy of the complex silicates may be estimated by the addition of the entropies of complex oxides [11]. Hence, the entropy change in a dehydration reaction (ΔS dehydration) is approximated by the entropy of the H_2O in the fluid phase($S_{(H2O)f}$) minus the entropy of the H_2O in the solid phase (S_{H2O} = Ice):

$$\Delta S_{dehydration} = S_{(H2O)f} - S_{(H2O)S} = \text{Ice}$$

ΔS of dehydration at 350°C and 3.5 kbar is estimated an about 12 cal / mol. deg. So far as the compositions of constituent minerals are fixed in this model system , the change of slopes, caused by changes of ΔS and ΔV with the P-T conditions for estimated errors in them are insignificant . Therefore, the invariant reaction lines are straight in P-T space. Although an invariant line of solid- solid reaction is usually a straight line with small positive slope in the P-T field, this paper regards it as a straight line parallel to the temperature axis, i.e. dP/dT = 0 as assumption of $\Delta S = 0$ in the case of the solid-solid reaction. A petrogenetic grid based on the Korzhinsky and Schreinemakers' methods is composed of invariant points and univariant reaction lines radiating from invariant points. As invariant circuit proposed by Hirajima [13] was used to construct the petrogenetic grids. By this procedure, three independent petrogenetic girds as follows are obtained (Figs. 3a,b,c).

1. [Bru]-[Clin]-[Pmp]-[Sps]-[Ky]
2. [Su]-[Tlc]-[Pi]
3. [Su]-[Ky]-[Phl]-[Clin]

Table 4. Characteristic assemblages of highly oxidized Mn-quartzites from Sanbagawa in central Shikoku and Andros and Evvia (after Izadyar [17] and Reinecke [32])

Mineral Name	Abb.	Formula	Volume	Entropy
Sursassite	Su	$Mn^{2+}{}_4Al_4Mn^{3+}MgSi_6O_{21}(OH)_7$	28.3	0.73
Pumpellyite	Pmp	$Ca_4Al_2Mn^{3+}{}_3Mg_{0.5}Mn^{2+}{}_{0.5}Si_6O_{21}(OH)_7$	29.55	0.63
Piemontite	Pi	$Ca_2Al_2Mn^{3+}Si_3O_{12}(OH)$	13.82	0.3
Spessartine	Sps	$Mn^{2+}{}_3Al_2Si_3O_{12}$	11.79	0.31
Braunite	Bru	$Mn^{2+}Mn^{3+}{}_6SiO_{12}$	12.51	0.42
Clinochlore	Clin	$Mg_5Al_2Si_3O_{10}(OH)_8$	21.09	0.421
Talc	Tlc	$Mg_3Si_4O_{10}(OH)_2$	13.63	0.26
Phlogopite	Phl	$KMg_3Si_3AlO_{10}(OH)_2$	14.96	0.35
Kyanite	Ky	Al_2SiO_5	4.41	0.08
Muscovite	Ms	$KAl_2Si_3AlO_{10}(OH)_2$	14.08	0.289
Quartz	Qtz	SiO_2	2.27	0.044
Water	H_2O	H_2O	1.98	0.19

Table 5. Invariant points, univariant assemblage and univariant reaction in the system

Invariant Point	Univariant Assemblage	Univariant Reaction
[Sps]	Clin + Tlc + Ky + Pmp + Su + Bru + Pi	R-1, R-9, R-14, R-18
[Pi]	Clin + Tlc + Ky + Pmp + Su + Bru + Sps	R-1, R-2, R-4, R-5
[Bru]	Clin + Tlc + Ky + Pmp + Su + Pi + Sps	R-1, R-8, R-16, R-17
[Pmp]	Clin + Tlc + Ky + Bru + Su + Pi + Sps	R-1, R-2, R-4, R-5
[Clin]	Pmp + Tlc + Ky + Bru + Su + Pi + Sps	R-5, R-11, R-15, R-16, R-18
[Tlc]	Pmp + Clin + Ky + Bru + Su + Pi + Sps	R-2, R-3, R-9, R-10, R-11, R-12
[Phl]	Tlc + Clin + Ky + Bru + Su + Pi + Sps	R-1, R-2, R-4, R-5
[Ky]	Tlc + Clin + Pmp + Bru + Su + Pi + Sps	R-4, R-6.R-10, R-13, R-14, R-15
[Su]	Tlc + Clin + Pmp + Bru + Ky + Pi + Sps	R-2, R-3, R-9, R-10, R-11, R-12

Table 6. Stoiqumetric univariant reactions

Reaction No.	Univariant Reaction
R-1	$3Clin + 14Qtz = 5Tlc + 3Ky + 7H_2O$
R-2	$90Su = 18Clin + 47Ky + 115Sps + 15Bru + 79 + Qtz + 243H_2O$
R-3	$109Ky + 90Pmp = 9Clin + 180Pi + 10Sps + 15Bru + 37Qtz + 189H2o$
R-4	$47Tlc + 54Su = 39Clin + 69Sps + 9Bru + 179Qtz + 80H_2O$
R-5	$18Su + Qtz = 6Tlc + 13Ky + 23Sps + 3Bru + 57H_2O$
R-6	$60Clin + 54Pmp + 283Qtz = 109Tlc + 108Pi + 6Sps + 9Bru + 266H_2O$
R-7	$20Ky + 18Pmo + Qtz = 3Tlc + 36Pi + 2Sps + 3Bru + 42H_2O$
R-8	$3Clin + 52Ky + 35Sps + 30Pmp + 14Qtz + 18H_2O = 60Pi + 30Su$
R-9	$289Ky + 230Pmp = 19Clin + 460Pi + 35Bru + 20Su + 77Qtz + 429H_2O$
R-10	$218Su + 94Pmp = 53Clin + 188Pi + 289Sps + 52Bru + 230Qtz + 786H_2O$
R-11	$53Ky + 19Sps + 36Pmp + Qtz = 72Pi + 3Bru + 18Su + 27H_2O$
R-12	$4.0Su + Pmp = Clin + Sps + 5.5Ky + 2.9Bru + 2.5Pi + 11.1Qtz + 2.25H_2O$
R-13	$2.2Clin + 1.33Sps + Pmp + 109Qtz = 3.5Tlc + Su + 2.5Pi + 2.5H_2O$
R-14	$7.6Clin + 3.75Pmp + 41.4Qtz = 12.9Tlc + Bru + Su + 9.37Pi + 36.4H_2O$
R-15	$10Su + 10Pmp = 5Tal + 7.8Bru + 25Pi + 5Sps + 2.2Qtz + 52.5H_2O$
R-16	$7.3Tlc + 15.5Ky + 10Pmp + 15.7H_2O + 18.3Qtz = 13Su + 25Pi$
R-17	$2.5Clin + 1.5Sps + Pmp + 11.5Qtz = 4Tlc + Su + 2.5Pi + 4.75H_2O$
R-18	$70Ky + 40Pmp + 53.2Qtz = 3.3Tlc + 10Su + 100Pi + 0.1Bru + 46.7H_2O$

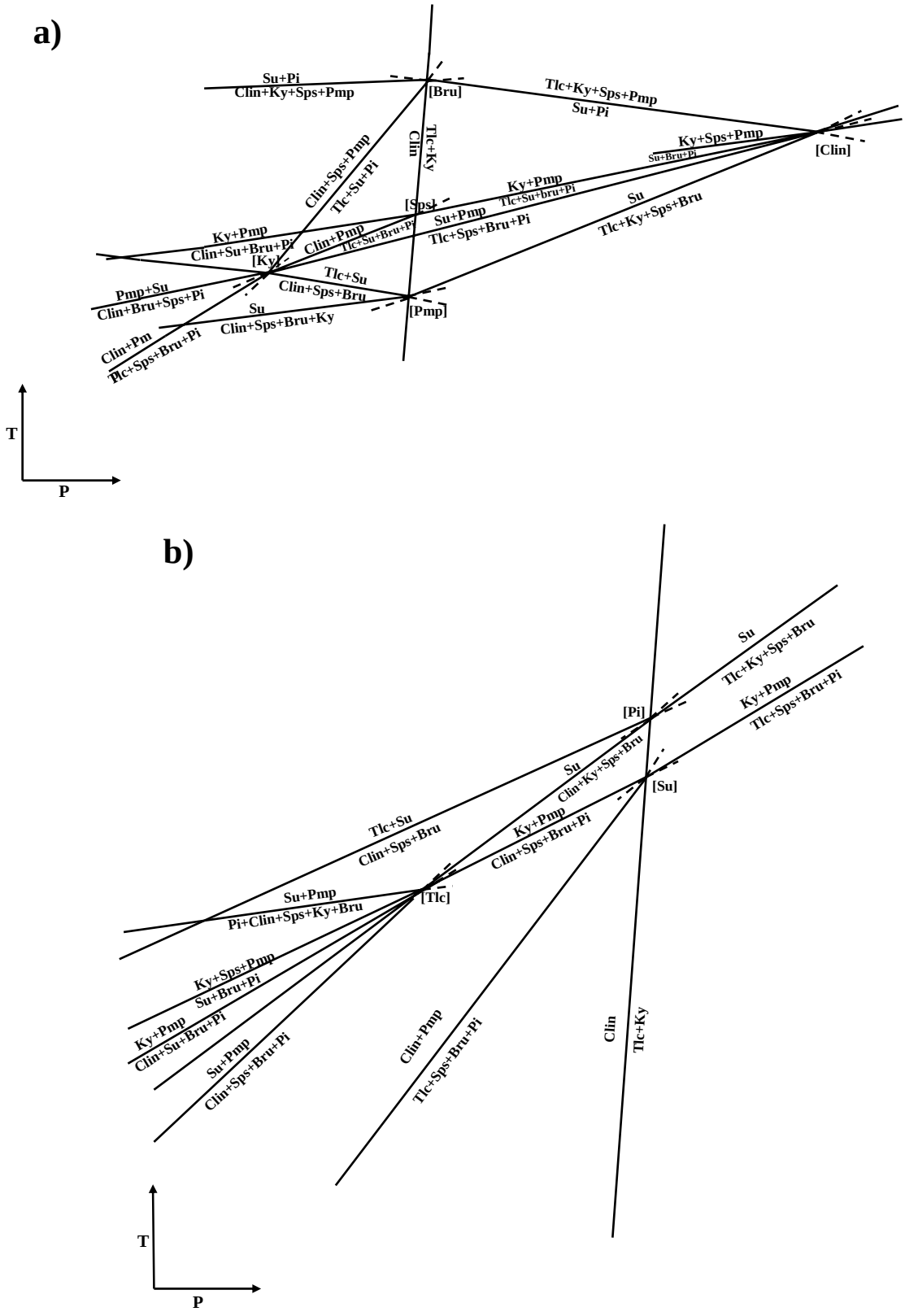

Figure 3. Petrogenetic girds for piemontite, braunite, surssasite, talc, clinochlore, phlogopite, pumpellyite, kyanite and spessartine with excess muscovite, quartz and water. a) [Clin] - [Pmp] - [Ky] - [Bru] - [Sps]; b) [Tlc] - [Su] - [Pi]; c) [Su] - [Ky] - [Phl] - [Clin].

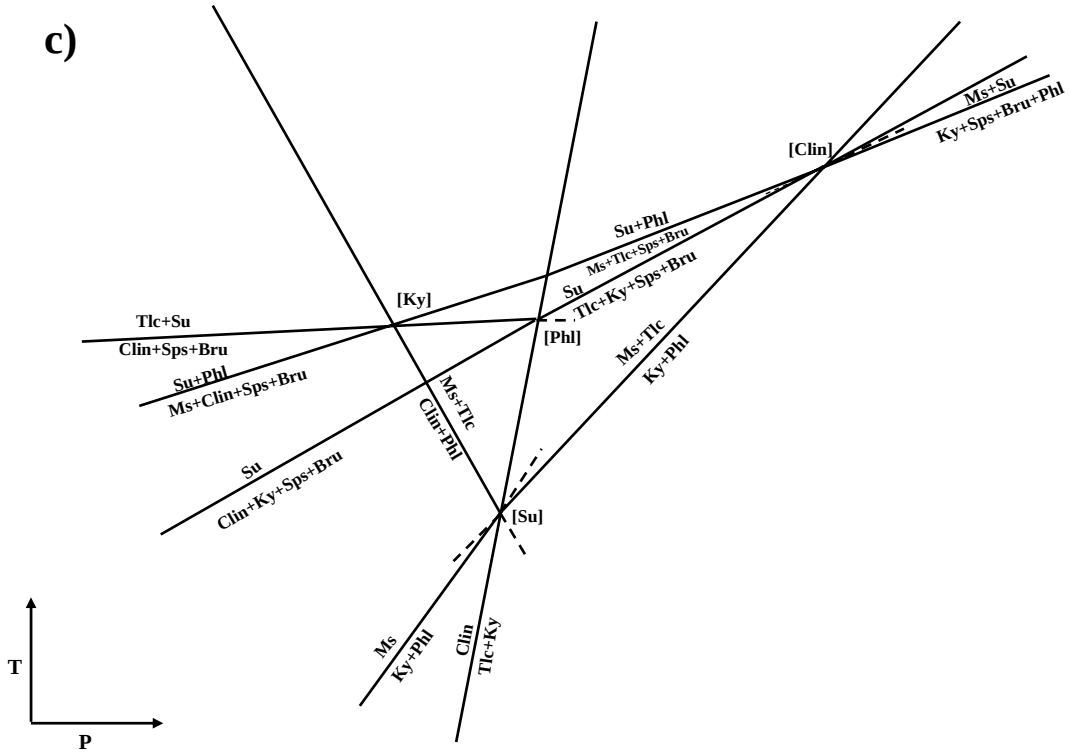

Figure 3. Continued.

Of three different orientations possible, Figure 3b presents the net with the minimum of inconsistencies in the sign of slope and in the position of the higher entropy assemblage. In the net, assemblage of sursassite + braunite + piemontite is stable at low temperature while assemblage containing piemontite, spessartine and braunite are plotted in the higher temperature. Sursassite metastable space is divided by the

Clin = Tlc+Ky and Clin+Pmp = Tlc+Sps+Bru+Pi

univariant lines into three areas; piemontite + braunite + spessartine + chlorite in the lowest, with talc in the medium and with kyanite in the highest part of the space. Preservation of the fo_2 can be seen by the stability of the Mn^{2+}–silicate phases in Su + Pi + Bru, Clin + Sps + Pi + Bru, Tlc + Clin + Sps + Pi + Bru and Tlc + Ky + Sps + Pi + Bru assemblages.

Considering the chemographic relationships in petrogenetic gird (Fig. 3b), it can vividly be concluded that highly oxidized Mn-Ca–Al–silicates in blueschist facies divided into three grades based on the relevant temperature:

low temperature assemblage: Su+Pmp+Clin+Bru+Pi

medium temperature assemblage: Clin+Sps+Bru+Pi

high temperature assemblage: Tlc+Sps+Bru+Pi

5. Discussion

In the following discussion, the phase relations obtained by Korzhinsky and Schrienemakers' methods for highly oxidized Mn-Ca-Al-silicates in blueschits facies have been applied to natural assemblages of Sanbagawa, Andros and Evvia. As mentioned, piemontite quartzites and braunite quartzites of Evvia contain sursassite, braunite, chlorite and piemontite [32], therefore, by proposed model they could be placed in low-temperature side of blueschist facies while those samples from Andros which include piemontite, spessartine, braunite, chlorite [32] are located in medium temperature part of blueschist facies and finally, piemontite-quartz schists of Sanbagawa which are mainly composed of piemontite, spessartine, talc, chlorite are placed in high-temperature side of the constructed net (compare the mentioned pressure and temperature for the Evvia, Andros and Sanbagawa respectively; T < 400°C, T ≈ 450°C and T > 450°C) [31-33]. Also, there are textural evidences from natural assemblages for the boundary reactions among low, medium and high temperature of blueschist facies in the proposed net. On Evvia and more rarely on Andros, some samples contain surssasite as well as spessartine besides piemontite, braunite, and quartz. In these rocks, however, surssasite is commonly replaced by spess-

artine implying that both minerals are not compatible and newly formed fine-grained spessartine invades surssasite with lobate grain boundaries and more rarely, spessartine forms prismatic pesudomorphs after surssasite (Fig. 4). Textural relationships suggest that the following reaction is responsible for the decomposition of sursassite in the presence of braunite [32]:

surssasite + braunite + quartz ==

spessartine + clinochlore + hematite + H_2O + O_2

Breakdown of surssasite appears not to be restricted to braunite-bearing assemblages, but is also observed in braunite-free piemontite-hematite quartzites. Reaction textures are similar to those in braunite-bearing assemblages and can be described by the net-transfer reaction [32]:

Surssasite + $Mn^{2+}Fe^{3+}_{-1}$ [piemontite, hematite]

+ hematite + quartz == spessartine

+ chlorite + H_2O + O_2

The P-T slops of the mentioned reactions calculated from molar volumes and entropies of relevant endmember phases are positive. Thus increasing temperature could favor the more dehydrated spessartine-bearing assemblage. On the other hand, calculated petrogenetic gird show highly oxidized, Mn-Al-Ca-rich quartzites and schists metamorphosed at higher grades than surssasite-pumpellyite-bearing ones usually contain assemblages with spessartine, piemontite, braunite and clinochlore, therefore, the low-T stability limit of spessartine + chlorite + quartz + piemontite is defined by the reactions such as:

surssasite + pumpellyite == spessartine

+ piemontite + chlorite + quartz + H_2O + O_2

This reaction is similar to mentioned reaction for natural assemblages obtained from Evvia and Andros.

In the Sanbagawa, texturally, spessartine containing many inclusions of piemontite and braunite does not occur as a fine-grained matrix mineral but only occurs as inclusion in albite porphyroblasts (Fig. 5). Textural relations also indicate that braunite occurs as inclusion in spessartine or as matrix mineral close to the piemontite, therefore, piemontite and braunite coexist. The partitioning of Mn^{3+}, Fe^{3+} and Al between piemontite and braunite confirms the assumption of their coexistence. Distribution coefficients have been calculated by the equations [18]:

$K_{D(Al\text{-}Mn)}=(X_{Al}/X_{Mn})_{Pi} / (X_{Al}/X_{Mn})_{Br}$, X_{Al}=Al/Al+Mn

$K_{D(Fe\text{-}Mn)}=(X_{Fe}/X_{Mn})_{Pi}/(X_{Fe} / X_{Mn})_{Br}$, X_{Mn}=Mn/Mn +Fe

and showing that relative to braunite, piemontite is enriched in Al and Fe^{3+} and depleted in Mn^{3+}. From the textural observations it is concluded that spessartine may be formed through a reaction involving piemontite and braunite.

The P-T slops of piemontite breakdown reaction to spessartine calculated from molar volumes and entropies of relevant endmember phases is positive and indicate that spessartine-bearing assemblage is restricted to higher temperature as was shown in proposed gird.

In the piemontite-quartz schists from Sanbagawa, chlorite and phengite are common but talc is restricted to medium and higher grade zones. Also phlogopite only occurs as rim of phengite in the garnet zone [17]. This observed mineral assemblage indicate that chlorite-bearing and talc-bearing assemblages could be related by following reaction:

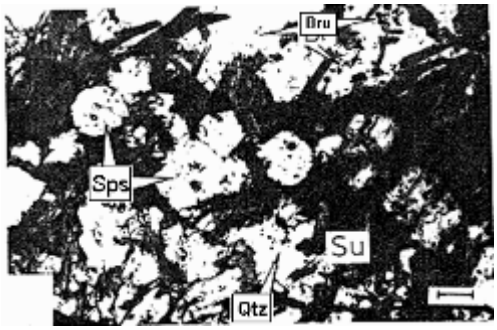

Figure 4. Photomicrograph of growth of spessartine (Sps) from intimately intergrown surssasite (Su) + braunite (Bru) + quartz (Qtz) in quartzites from southern Evvia (after Reinecke [32]). 1 Nicol. Scale bar = 50 μm.

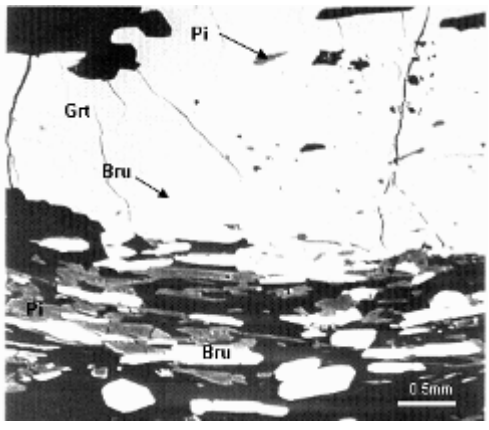

Figure 5. Back scattered electron image of spessartine (Sps), piemontite (Pi) and Braunite (Bru) from Sanbagawa piemontite-quartz schist.

chlorite + phlogopite == phengite + talc

This reaction has been investigated both experimentally and thermodynamically [17,27] and show that talc-bearing assemblage is stable on higher temperature than chlorite-bearing ones, the same conclusion as obtained from proposed petrogenetic gird.

The constructed petrogenetic gird can be applied to any highly oxidized Mn-Al-Ca-silicate bearing quartzite/schists of blueschist type metamorphism to determine the temperature equilibration. Mitchell and Corey [28] reported mineral assemblage of quartz + Sursassite + braunite in quartzite, Log Angeles County, California and determined low-grade blueschist facies for metamorphic condition. By using of the proposed net, the same result can be obtained.

Chopin [7] while studing piemontite quartzite in Gran Paradiso massif, French Alps, reported quartz + piemontite + spessartine + braunite + hematite + phengite + talc + clinochlore + phlogopite assemblage and concluded that they are formed under high-grade blueschist type of metamorphism. The same result can be gained by proposed petrogenetic gird. Looking at the published data other than mentioned above [25,9,1,8] show correspondence between different natural assemblages in response to variable physical conditions and their relative stability relations predicted from Korzhinsky and Schreinemakers' analysis.

6. Concluding Remarks

The following results were obtained from the analysis of paragenesis of Mn-silicate bearing quartzites and schists in highly oxidized blueschist facies by using Korzhinsky and Schrienemakers' methods:

1- Studying phase relationships of highly oxidized Mn-silicate bearing rocks will eventually widen the use of rocks easily recognized in the field from the mere condition of structural markers to that of indicators of equilibration within the high-pressure facies sequence.

2- The analysis of phase compatibility in the system $AMn^{2+}Mn^{3+}CMKSH$ containing piemontite, spessartine, braunite, surssasite, pumpellyite, phlogopite, clino-chlore, talc and kyanite with excess muscovite, quartz and water, points to three different assemblages: low temperature assemblages containing surssasite, pumpe-llyite, clinochlore and piemontite; medium temperature assemblage containing clinochlore, spessartine, braunite and piemontite and high temperature assemblage including talc, spessartine, braunite and piemontite.

3- Application of the obtained model to natural assemblages from Sanbagawa metamorphic belt, Japan and Andros and Evvia islands, Greece, show that samples from Evvia are in low temperature part of blueschist facies and those from Andros are in medium temperature and finally samples from Sanbagawa are placed in high temperature part of blueschist facies.

References

1. Abraham K. and Schreyer W. A talc-phengite assemblage in piemontite schists from Brezovica, Serbia, Yougoslavia. *Journal of Petrology*, **17**: 421-439 (1976).
2. Abs-Wurmbach I., Peters T., Langer K., and Schreyer W. Phase relations in the system Mn-Si-O. An experimental and petrological study. *Neues Jahrb Mineral Abh*, **146**: 258-279 (1983).
3. Anastasiou P. and Langer K. Synthese and Stabilität von piemontite, $Ca_2Al_{3-p}Mn_p^{3+}(Si_2O_7/O/OH)$. *Fortschr Mineral 54*, Beih **1**: 3-4 (1976).
4. Anastasiou P. and Langer K. Synthesis and physical properties of piemontite $Ca_2Al_{3-p}Mn^{3+}{}_p(Si_2O_7/SiO_4/O/OH)$. *Contributions to Mineralogy Petrology*, **60**: 225-245 (1977).
5. Banno S. and Sakai C. Geology and metamorphic evolution of the Sanbagawa metamorphic belt, Japan. In: Daly J.S., Cliff R.H., and Yardley B.W.D. (Eds), Evolution of metamorphic belts. *Geological Society Special Publication*, **43**: 519-532 (1989).
6. Burnham C.W., Holloway J.R., and Davis N.F. Thermodynamic properties of water to 1000°C and 10000 bars. *Memorial of Geological Society of America, Special Paper*, 132 (1969).
7. Chopin C. Talc-phengite: a widespread assemblage in high-grade pelitic blueschists of the Western Alps. *Journal of Petrology*, **22**: 628-650 (1981).
8. Cortesogno L., Lucchetti G., and Penco A.M. Le mineralizzazioni a manganese nei diaspri delle ofioliti Liguri : mineralogiae genesi. *Rend.Soc. Ital. Mineral. Petrol.*, **35**: 151-197 (1979).
9. Dal Piaz G.V., Di Battistini G., Kienast J.R., and Venturelli G. Mangaiferous quartzitic schists of the piemontite ophiolite nappe in the Valsesia-Valtournanche area (Italian Western Alps). *Mem. Sci. Geol. Padova*, **32**: 1-24 (1979).
10. Enami M. Petrology of pelitic schists in the oligoclase-biotite zone of the Sanbagawa metamorphic terrain, Japan :phase equilibria in the highest grade zone of a high-pressure intermediate type of metamorphic belt. *Journal of Metamorphic Geology*, **1**: 141-161 (1983).
11. Fyfe W.S., Turner F.J., and Verhoogen J. Metamorphic reactions and metamorphic facies. *Memorial of Geological Society of America*, **73**: 21-51 (1985).
12. Higashino T. Biotite zone of Sanbagawa metamorphic terrain in the Siragayama area, central Shikoku, Japan. *Journal of Geological Society of Japan*, **81**: 653-670 (1975).
13. Hirajima T. Petrological study of the Sanbagawa metamorphic belt in the Kanto mountains, Japan, *Ph.D. Thesis*, Kyoto University, Unpublished 260 p. (1983).
14. Holland T.J.B. and Powell R. An enlarged and updated internally consistent thermodynamic dataset with uncertainties and correlations: the system K_2O-MnO-

Fe_2O_3-Al_2O_3-TiO_2-SiO_2-C-H_2-O_2. *Journal of Metamorphic Geology*, **8**: 89-124 (1990).
15. Hsu L.C. Selected phase relationships in the system Al-Mn-Fe-Si-O-H : a model for garnet equilibria. *Journal of Petrology*, **9**: 40-83 (1968).
16. Izadyar J., Tomita k., and Shinjoe H. Geochemistry and origin of piemontite-quartz schists in the Sanbagawa Metamorphic Belt, central Shikoku, Japan, *Journal of Asian Earth Sciences*, **21**: 711-730 (2003).
17. Izadyar J., Hirajima T., and Nakamura D. Talc-phengite assemblage in piemontite-quartz schist of the Sanbagawa metamorphic belt, central Shikoku, Japan. *The Island Arc*, **9**: 145-156 (2000).
18. Izadyar J. Chemical composition of piemontite and reaction relations of piemontite and spessartine in piemontite-quartz schists of central Shikoku, Sanbagawa metamorphic belt, Japan. *Schweizerische Mineralogische und Petrographische Mitteilungen*, **80**: 199-210 (2000).
19. Kawachi Y., Grapes R.H., Coombs D.S., and Dowse M. Mineralogy and petrology of a piemontite-bearing schist, Western Otago, New Zealand. *Journal of Metamorphic Geology*, **1**: 353-372 (1983).
20. Keskinen M. Petrochemical investigation of the Shadow lake piemontite zone, Eastern Sierra Nevada, California. *American Journal of Science*, **281**: 896-921(1981).
21. Keskinen M. and Liou J.G. Synthesis and stability relations of Mn-Al piemontite, $Ca_2MnAl_3Si_3O_{12}(OH)$. *American Mineralogist*, **64**: 317-328 (1979a).
22. Keskinen M. and Liou J.G. Experimental evidence on the effect of Fe and Mn on piemontite and epidote stability. Eos. *American Geophysical Union Transaction*, **60**: 965 (1979b).
23. Kretz R. Symboles for rock-forming minerals. *American Mineralogist*, **68**: 277-279 (1983).
24. Martin S. and Lombardo B. Sursassite, spessartine, piemontite in Fe-Mn metacherts from Lago Bleu, upper Val Varaita (western Alps). *Museo Regionale Di Scienze Naturali*, **13**: 103-126 (1995).
25. Martin-Vernizzi S. La mine de Praborna (Vald' Aoste, Italie): une série manganésifére métamorphisée dans le facies éclogite. These 3éme cycle. Université Pierre et Marie Curie, paris, 215 p. (1982).
26. Massone H.J. Phengite: eine experimentelle Untersuchung ihres Druck-Temperatur-Verhaltens im system K_2O-MgO-Al_2O_3-SiO_2-H_2O. Diss Ruhr-Universitat Bochum, 211 (1981).
27. Massone H.J. and Schreyer W. The stability of the high-pressure assemblage talc-phengite, and two new phengite geobarometers. *Euro. J. Mineral.*, **1**: 340-391 (1989).
28. Mitchell R.S. and Corey A.S. Braunite and sursassite from Los Angeles county, California. *Miner. Rec.*, **4**: 290-293 (1973).
29. Mottana A. Melting of spessartine at high pressure. *Neues Jahrb Mineral*, Monatsh, 256-271 (1974).
30. Mottana A. Blueschist facies metamorphism of manganiferous cherts: A review of the alpine occurrences. *Geological Society of America*, **164**: 267-296 (1986).
31. Reinecke T. Mineralogie und petrologie der mangan-und eisenreichen metasedimente von Andros, Kykladen, Griechen Land. Dissertation, Technische universität Braunschweig, 256 p.(1983).
32. Reinecke T. Phase relationships of sursassite and other Mn-silicates in highly oxidized low-grade, high-pressure metamorphic rocks from Evvia and Andros islands, Greece, *Contributions to Mineralogy and Petrology*, **94**: 110-126 (1986).
33. Reinecke T. Crystal chemistry and reaction relations of piemontites and thulites from highly oxidized low grade metamorphic rocks at Vitali, Andros island, Greece. *Contributions to Mineralogy and Petrology*, **93**: 56-76 (1986).
34. Wallis S.R., Banno S., and Radvance M. Kinematics, Structure and relationship to metamorphism of east-west flow in the Sanbagawa belt, Southwest, Japan. *The Island Arc*, **1**: 176-185 (1992).
35. Zen E-an. Construction of pressure-temperature diagrams for multicomponent system after the method of Schreinemakers: A geometric approach. *U.S. Geological Survey Bulletin*. 1225-56 (1966).